

# Laboratori Nazionali di Frascati

Submitted to Europhys. Letters

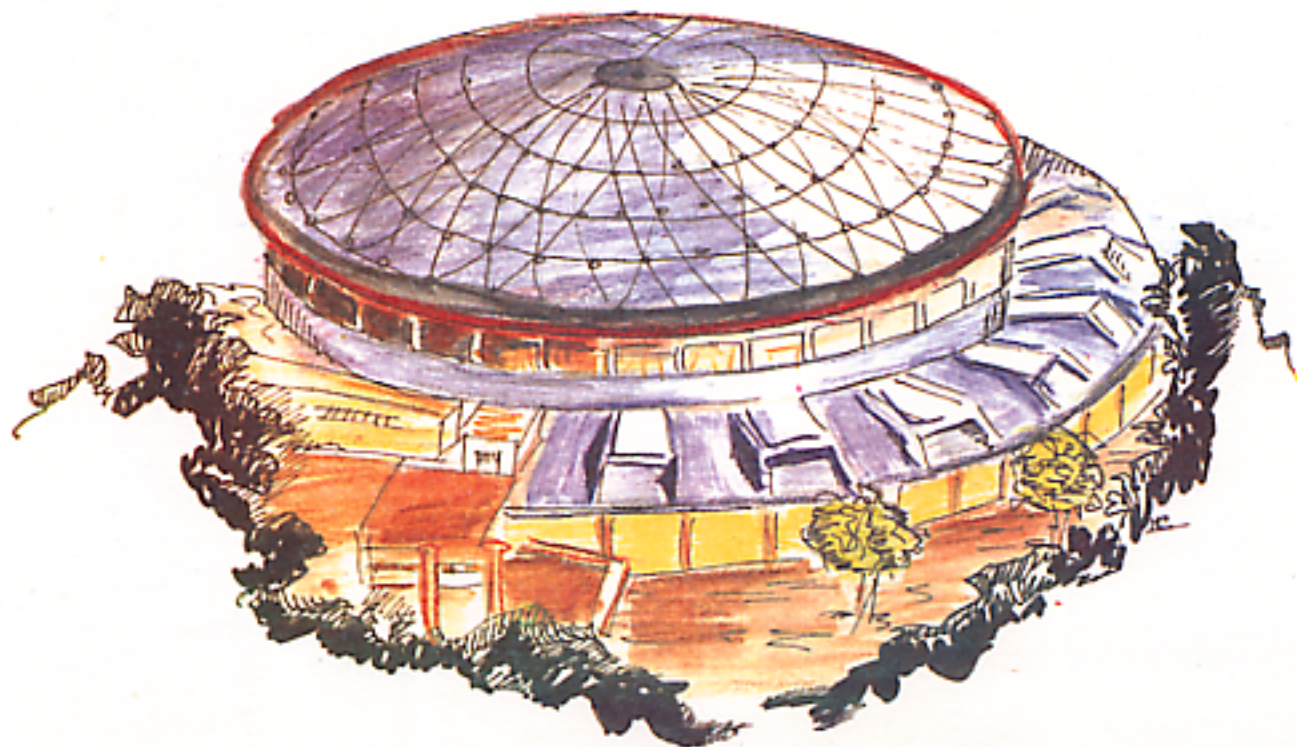
LNF-94/016 (P)

18 Marzo 1994

J. Chaboy, A. Marcelli, L.M. Garcia, J. Bartolomé, M.D. Kuz'min,  
H. Maruyama, K. Kobayashi, H. Kawata, T. Iwazumi:

**X-RAY CIRCULAR MAGNETIC DICHROISM AS A PROBE OF  
SPIN REORIENTATION TRANSITIONS IN  $Nd_2Fe_{14}B$  AND  
 $Er_2Fe_{14}B$**

PACS.: 75.25.+z; 78.20.Ls; 75.50.Bb; 78.70.Dm



Servizio Documentazione  
dei Laboratori Nazionali di Frascati  
P.O. Box, 13 - 00044 Frascati (Italy)

**X-RAY CIRCULAR MAGNETIC DICHROISM AS A PROBE OF SPIN  
REORIENTATION TRANSITIONS IN  $Nd_2Fe_{14}B$  AND  $Er_2Fe_{14}B$**

J. Chaboy<sup>1,\*</sup>, A. Marcelli<sup>1</sup>, L. M. García<sup>2</sup>, J. Bartolomé<sup>2</sup>,  
M.D. Kuz'min<sup>2</sup>, H. Maruyama<sup>3</sup>, K. Kobayashi<sup>3</sup>,  
H. Kawata<sup>4</sup> and T. Iwazumi<sup>4</sup>

<sup>1</sup>*I. N. F. N., Laboratori Nazionali di Frascati - Casella Postale 13, 00044 Frascati, Italy*

<sup>2</sup>*Instituto de Ciencia de Materiales de Aragón, 50009 Zaragoza, Spain*

<sup>3</sup>*Department of Physics, Faculty of Science, Okayama University, Japan*

<sup>4</sup>*Photon Factory, National Laboratory for High Energy Physics, 1-1 Oho, Tsukuba, Japan*

We present the first experimental observation of spin reorientation phase transitions (SRT) with the X-Ray Circular Magnetic Dichroism (XCMD) technique. The XCMD signal, related to the projection of the rare earth moment on the direction of the x-ray beam, has been measured as a function of temperature for both, a first-order SRT in  $Er_2Fe_{14}B$  (abrupt reorientation by  $90^\circ$ ) and a second-order one in  $Nd_2Fe_{14}B$ , (continuous tilt of the magnetization from the c-axis). The feasibility of this technique to study SRTs is demonstrated, resulting in a better understanding of the magnetic behavior of intermetallic compounds exhibiting coexistence of itinerant and localized magnetism.

The  $RE_2Fe_{14}B$  compounds (RE= Nd, Ho, Er, Tm and Yb) are known to undergo changes in the orientation of the easy axis magnetization direction (EMD). As the temperature is lowered, the magnetic structure with the EMD parallel to the c-axis, gives way to other structures: in  $Er_2Fe_{14}B$ ,  $Tm_2Fe_{14}B$  and  $Yb_2Fe_{14}B$  the EMD becomes abruptly parallel to the a-axis, whereas in  $Nd_2Fe_{14}B$  and  $Ho_2Fe_{14}B$  the EMD tilts from the c-axis towards [110] by an angle  $\theta_t$  which varies continuously with temperature[1]. Such transformation is called Spin Reorientation Transition (SRT) and for each compound it occurs at a specific transition temperature  $T_s$ . Notwithstanding the fact that the behavior of the bulk magnetization has been well determined, the evolution of the magnetic moments on the microscopic scale is less understood, specially in the case of  $Nd_2Fe_{14}B$  and  $Ho_2Fe_{14}B$ , where in the low-temperature phase the RE and Fe moments can be considerably non-collinear. Although the  $RE_2Fe_{14}B$  compounds have been thoroughly studied by many experimental techniques, (in particular  $Nd_2Fe_{14}B$  was studied by  $^{145}Nd$  [2],  $^{57}Fe$  Mössbauer spectroscopies [3], X-ray Resonance Exchange Scattering (XRES) [4] and neutron diffraction[5]) no general agreement on the mutual orientation of the RE and Fe moments has been reached so far.

The X-Ray Circular Magnetic Dichroism (XCMD) technique appears to be a unique probe to study the magnetism of complex alloys allowing direct measurement of the spin-dependent absorption cross section on a given atomic specie in a material with net magnetization.[6, 7] Moreover, due to the dipolar selection rules, this spectroscopy yields directly the spin polarization of empty states of a given symmetry near the Fermi level by selecting the initial state. In intermetallic compounds, it is worth pointing out the important role played by the conduction electrons in the interaction between the Transition Metal (TM) and RE atoms, which tunes the magnetic properties. These conduction electrons are very difficult to characterize magnetically since their response to the magnetic probes is generally small compared to the prominent signal given by the narrow bands. Thus, the capability of XCMD to probe directly the rare earth  $5d$  band is of fundamental interest. However, despite the growing interest motivated by the results obtained in the last years by XCMD, to date there is no published report about its feasibility to study magnetic phase transitions other than the ferro(i)magnetic ordering transition.

In this work, XCMD is for the first time applied to study magnetic order-order phase transitions. The feasibility of this technique to study SRT is demonstrated, resulting in a better understanding of the magnetic behavior of intermetallic compounds exhibiting coexistence of itinerant and localized magnetism.

To this end we chose two different paradigmatic cases:  $Er_2Fe_{14}B$ , which undergoes an abrupt first order transition at  $T_s = 315$  K, and  $Nd_2Fe_{14}B$ , which has a second-order transition at  $T_s = 135$  K.[1] The samples were prepared by melting a sandwich of the starting elements in a cold crucible, using the high-frequency levitation technique. After milling, the powder was embedded in an epoxy glue at  $T = 350$  K under a magnetic field of 1.5 T. The samples were cut into thin plates with the

plane along the alignment direction. The misorientation of the grains was determined by magnetization measurements to be of the order of a few degrees. This procedure guaranties that most of the grains have their crystallographic c-axes parallel to each other. We verified by measuring the magnetic hysteresis cycle that, when reversing a 0.6 T external field, full reversion of the magnetization takes place. This guaranties single magnetic domain conditions in the XCMD experiments described below.

Experiments were performed at the National Laboratory for High Energy Physics (KEK) on the Accumulator ring of TRISTAN at the beamline AR NE1.[8] Left circular polarized x-ray radiation, emitted by the Elliptic Multipole Wiggler (EMPW), was used with a degree of polarization of more than 0.6 after monochromatization.

The beamline was equipped with a Si(111) fixed-exit-beam double crystal monochromator. Higher harmonics rejection both at the energy of the  $K$ -edge of iron and at the  $L_2$ - edge of Nd was obtained by detuning the two crystals of the monochromator[9] by 6 arcsec from the Bragg angle. Sagittal focusing was also used, both to reduce the spot size on the sample position and to improve the S/N ratio. The energy resolution  $\Delta E/E$  in this condition was estimated to be about  $2 \times 10^{-4}$ . [10] The measurements were performed at different fixed temperatures from 300 K to 325 K for the  $Er_2Fe_{14}B$  sample and from room temperature down to 50 K for  $Nd_2Fe_{14}B$  using a closed-cycle He cryostat.

The XCMD spectra were recorded by reversing the sample magnetization for a fixed polarization of the incoming radiation. In our experimental setup a magnetic field of 0.6 T was applied parallel to the plane of the sample at  $45^\circ$  to the incident beam and reversed twice for each energy value. To improve the total flux, the incident angle was a few degrees less than  $45^\circ$ , and the c-axis was in the incident plane. The transmission intensity  $I$  and the incident beam intensity  $I_0$  were measured by two separate ionization chambers. The data were accumulated every 2 seconds in order to minimize any time dependent drift. Multiple scans were made (6-12 acquisitions) to reduce the statistical uncertainty to about  $2 \times 10^{-4}$ .

The spin-dependent absorption coefficient  $\mu_c$  is given by the difference of the absorption coefficient for parallel,  $\mu^+$ , and antiparallel,  $\mu^-$ , orientation of the photon spin and the magnetic field applied to the sample. The spectra were normalized to the averaged absorption coefficient at high energy,  $\mu_0$ , in order to eliminate the dependence of the absorption on the sample thickness so that  $\mu_c(E)/\mu_0 = (\mu^+(E) - \mu^-(E))/\mu_0$  corresponds to the adimensional spin-dependent absorption coefficient. The origin of the energy scale was chosen at the inflection point of the absorption edge. Because spin-polarized photoelectrons are excited in the photoabsorption process, the absorption probability is sensitive to the density of unoccupied final states with the same spin direction. Thus, within a one-electron framework and by introducing the difference of the density of empty states,  $\rho(E)$ , with spin polarization parallel ( $\uparrow\uparrow$ ) and antiparallel ( $\uparrow\downarrow$ ) to that of the photon spin, the normalized spin-dependent absorption can be expressed as  $\frac{\mu_c}{\mu_0} = K \frac{\Delta\rho}{\rho}(E) \cos\theta$ , where  $\Delta\rho(E) = \rho^{\uparrow\uparrow}(E) - \rho^{\uparrow\downarrow}(E)$ ,  $\theta$  is the angle between the local spin polarization and the x-ray wave vector and  $K$  is proportional

to both the rate of polarization of the excited photoelectron and the rate of circular polarization of the incident beam, the sign of  $K$  depending on the particular edge explored.[6, 11]

The room temperature XCMD spectra obtained at both the Fe  $K$ -edge and at the Nd  $L_2$ -edge in the case of  $Nd_2Fe_{14}B$  are shown in Fig. 1. In the case of the iron  $K$ -edge where the  $4p$  empty states are probed, the dichroic signal yields directly the sense of the magnetic moment on iron atoms relative to the net magnetization of the sample ( $K > 0$ ).[11] Comparison of the iron  $K$ -edge signal in  $Nd_2Fe_{14}B$  to that of elemental iron, shows a close similarity both in intensity and energy splitting between the spin-up and spin-down components. This result is in agreement with the proximity of the average Fe moment in  $Nd_2Fe_{14}B$  ( $\simeq 2.1\mu_B$ ) to that of elemental Fe ( $2.2\mu_B$ ).[1] Moreover, the similarity of the Fe- $4p$  density of states as probed by the photoelectron, see Fig. 1, indicates that the charge transfer from the rare earth to the conduction bands has no significant effect at the Fe sites.

The XCMD effect at the  $L_2$ -edge,  $K < 0$ , probes the spin polarization of the final  $d$ -states of the photoabsorbing atom; its positive sign indicating that the density of  $5d$ -down spins,  $\rho_{5d}^{\uparrow\downarrow}$ , is larger than the density of up spins,  $\rho_{5d}^{\uparrow\uparrow}$ , for the same energy above the Fermi level.[11] This result demonstrates that the average spin of the Nd  $5d$ -states is antiferromagnetically coupled to the Fe spin. On the other hand, since the intra-atomic  $4f - 5d$  positive exchange interaction renders the  $4f$  and  $5d$  rare earth spins parallel to each other,[12] one concludes that the mutual orientation of the Nd- $4f$  and Fe- $3d$  spins is antiparallel. Hence, because Nd is a light rare-earth,  $J = L - S$ , the Nd- $4f$  magnetic moment is ferromagnetically coupled to that of Fe. Indeed, Campbell proposed such a scheme to give account of the RE-TM interaction [13]. In the case of  $Nd_2Fe_{14}B$ , to our knowledge, this is the first direct verification of the  $5d - 3d$  antiferromagnetic coupling in the proposed  $4f - 5d - 3d$  coupling scheme. Moreover, the  $\Delta\rho$  profile directly probed by XCMD, shown in Fig. 1 changes sign, in agreement with previous electronic structure calculations[14, 15] which show that the Nd  $\rho_{5d}^{\uparrow\downarrow}$  exceeds  $\rho_{5d}^{\uparrow\uparrow}$  up to  $\simeq 8$  eV above the Fermi level, whereas the change of dominant spin polarized  $\rho_{4p}(E)$  of Fe takes place at a lower energy,  $\simeq 4$  eV. On the other hand, the existence of an induced  $5d$  magnetic moment opposite in sign to that of Fe agrees with the prediction obtained by means of self-consistent spin-polarized band structure calculations.[16]

The comparison of the XCMD signal at the  $L_2$ -edge of the rare earth recorded at different temperatures is reported in Fig. 2 for both the  $Nd_2Fe_{14}B$  and  $Er_2Fe_{14}B$  compounds. The temperature dependence of the XCMD signal does not suggest any change of the coupling sign with temperature, or at the SRT. In the case of  $Er_2Fe_{14}B$  the XCMD signal is zero at room temperature, when the magnetization is perpendicular to the  $c$ -axis and to the applied field and hence cannot be reversed by the latter, while it becomes suddenly negative as the transition temperature is reached,  $T_s = 315$  K. This is exactly the behavior expected for  $\frac{\mu_c}{\mu_0}$  when  $\theta_i$  turns from  $\pi/2$  to 0. On the other hand, in the case of  $Nd_2Fe_{14}B$  the amplitude of the dichroic

signal raises continuously as the temperature decreases.

The character of the transition can be studied by considering the integrated intensity of the XCMD, as shown in Fig. 3 as a function of temperature. Its abrupt change in  $Er_2Fe_{14}B$  agrees with the first-order nature of the magnetic transition. On the contrary, in  $Nd_2Fe_{14}B$  it grows in a continuous manner when cooling down through  $T_s$ , showing a rounded maximum at about  $T_m = 110$  K. This behavior reflects the fact that the tilting angle  $\theta_t$  increases continuously as the temperature decreases. Because of the strong exchange between the Nd 4f and 5d moments, the XCMD signal is expected to reflect the temperature dependence of the average projection of the Nd magnetic moment in the direction of the beam:  $\langle \mu_{Nd} \cos \theta \rangle = \mu_{Nd} (\cos \alpha \sin \theta_t \langle \cos \phi \rangle + \sin \alpha \cos \theta_t)$  where the orientation of the Nd moment is described by the spherical angles  $\theta_t$  and  $\phi$ , with the z-axis parallel to the sample c-axis and the x-axis perpendicular to the sample, so that the x0z plane is contained in the incident plane. It is important to notice that as the SRT sets on the EMDs of the ensemble of crystallites deviate from the common c-axis and form a cone with an opening angle  $\theta_t$ . The distribution of the EMDs within the cone is not necessarily uniform because in our experiment the applied field is not exactly parallel to the c-axis. This non-uniformity is reflected by a non-zero value of  $\langle \cos \phi \rangle$ .

To estimate the temperature dependence of this projection we may consider the available data on  $\mu_{Nd}$  and  $\theta_t$ . By means of  $^{145}\text{Nd}$  Mössbauer spectroscopy it was determined that the hyperfine field, related to the modulus of its magnetic moment, increased below  $T_s$  and the tilting angle augmented till  $36^\circ$ , slightly non-collinear with the Fe sublattice.[2] Moreover, from  $^{57}\text{Fe}$  Mössbauer experiments in a larger temperature range, a similar increase in the modulus was deduced indirectly through the tilting angle, which deviated much more from collinearity[3], as it was also found in a recent neutron diffraction investigation[5]. Furthermore, in a recent XRES experiment, the tilting angles of sites 4f and 4g in the structure were proposed to be different (one at each side of the EMD below  $T_s$ ).

So, assuming that  $\mu_{Nd} \propto H_{hf}$  and taking  $\theta_t(T)$  from Refs.[2, 3], we have scaled the projection  $\langle \mu_{Nd} \cos \theta \rangle$  on the XCMD data with  $\langle \cos \phi \rangle = 0.4$  and  $0.64$  as fit parameters, respectively. As can be seen in Fig. 3, this analysis explains satisfactorily the measured XCMD signal.

Finally, we present in Fig. 4 the temperature dependence of the Nd  $L_2$ -edge XANES spectra. Upon cooling down through  $T_s$  a sudden reinforcement of the white-line feature is evidenced as the SRT takes place, indicating an increase of the local density of 5d empty states at the Nd site. This effect, reflecting a higher localization of the 5d electrons, might be correlated with the observed increase of the Nd magnetic moment below  $T_s$ . Also the increase of the 5d-character of the empty states may associated to weakening of the 3d – 5d hybridization.

The remarkable similarity exhibited between the XCMD signal and the Mössbauer data demonstrates the feasibility of the XCMD technique to the study of SRT transitions. We conclude that this technique probes both the magnitude of the RE moment,

and orientation, through the projection of  $\mu_{Nd}$  on the x-ray beam direction. The servitude of measuring on a powder sample avoids us going further on the analysis, but from the error bars in Fig. 3 we can expect to be sensitive to non-collinear magnetic arrangements greater than  $15^\circ$ . Both the use of single crystal specimens and the optimization of the experimental setup could improve significantly this resolution.

We are indebted to T. Miyahara for his invaluable help during our time at KEK. We wish also to thank F. Itoh and H. Sakurai of Gunma University and K. Shimomi and H. Yamazaki of Okayama University for their precious help during experimental runs. This work has been performed with the approval of the Photon Factory Program Advisory Committee (Proposal N.91-215). One of us (J.Ch.) acknowledges an FPI grant of the Ministerio de Educación y Ciencia of Spain. This work was supported by DGICYT MAT91/487 and MAT93/0240C04 grants and by INFN.

REFERENCES

- \* Present Address: Departamento de Física de la Materia Condensada & Instituto de Ciencia de Materiales de Aragón, 50009 Zaragoza, Spain
- [1] For a review, J.F. Herbst, *Rev. Mod. Phys.* **63**, 819 (1991) and references therein.
  - [2] I. Nowik, K. Muraleedharan, G. Wortmann, B. Perscheid, G. Kaindl and N.C. Koon, *Solid State Comm.* **76**, 967 (1990).
  - [3] H. Onoedera, A. Fujita, H. Yamamoto, M. Sagawa and S. Hirosawa, *J. Mag. Mag. Mat.* **68**, 6 (1987); *J. Mag. Mag. Mat.* **68** 15 (1987).
  - [4] A. Koizumi, K. Namikawa, H. Maruyama, K. Mori and H. Yamazaki, *Jpn. J. Appl. Phys.* **32** 332 (1993).
  - [5] D. Fruchart, S. Miraglia, S. Obbade, B. Verhoef and P. Wolfers, *Physica B180&181*, 578 (1992).
  - [6] G. Schütz, W. Wagner, W. Wilhelm, P. Kienle, R. Zeller, R. Frahm and G. Materlik, *Phys. Rev. Lett.* **58**, 737 (1987).
  - [7] G. Schütz, M. Knulle, R. Wienke, W. Wilhelm, W. Wagner, P. Kienle and R. Frahm, *Z. Phys.* **B73**, 67 (1988).
  - [8] S. Yamamoto, H. Kawata, H. Kitamura, M. Ando, N. Saki and N. Shiotani, *Phys. Rev. Lett.* **62**, 2672 (1989).
  - [9] H. Kawata, T. Miyahara, S. Yamamoto, T. Shioya, H. Kitamura, S. Sato, S. Asaoka, N. Kanaya, A. Iida, A. Mikuni, M. Sato, T. Iwazumi, Y. Kitajima and M. Ando, *Rev. Sci. Instr.* **60**, 1885 (1989).
  - [10] T. Iwazumi, M. Sato and H. Kawata, *Rev. Sci. Instr.* **63**, 419 (1992).
  - [11] The empirical model used by G. Schütz et al. to derive  $\frac{\mu_c}{\mu_0}$  is physically appealing but qualitative. More recently, the same result has been discussed by Brouder and Hikam in a rigorous framework on the grounds of the multiple scattering XCMD theory. C. Brouder and M. Hikam, *Phys. Rev.* **B43**, 3089 (1991).
  - [12] Wm. R. Callahan, *J. Opt. Soc. Am.* **53**, 695 (1963)
  - [13] I.A. Campbell, *J. Phys.* **F2**, L47 (1972).
  - [14] W.Y. Ching and Z.G. Gu, *J. Appl. Phys.* **61**, 3718 (1987).
  - [15] S. S. Jaswal, *Phys. Rev.* **B41**, 9697 (1990).
  - [16] L. Nördstrom, B. Johansson and M.S.S. Brooks, *J. Appl. Phys.* **69**, 5708 (1991).



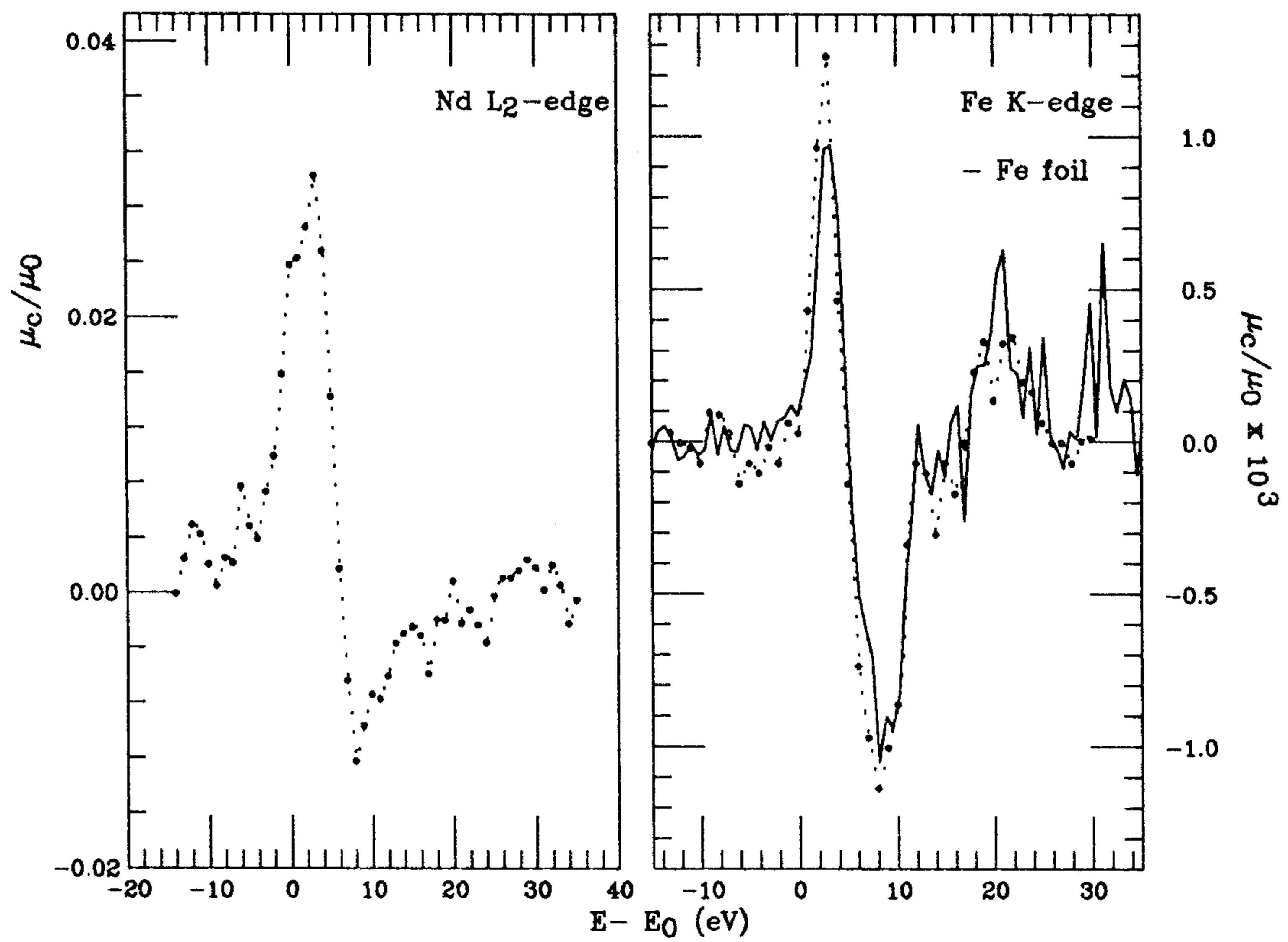


FIG. 1. XCMD signals at the  $L_2$ -edge of Nd (left panel) and at the iron  $K$ -edge in the  $Nd_2Fe_{14}B$  compound measured at room temperature. The solid line on left panel corresponds to the XCMD at the iron  $K$ -edge of elemental iron.

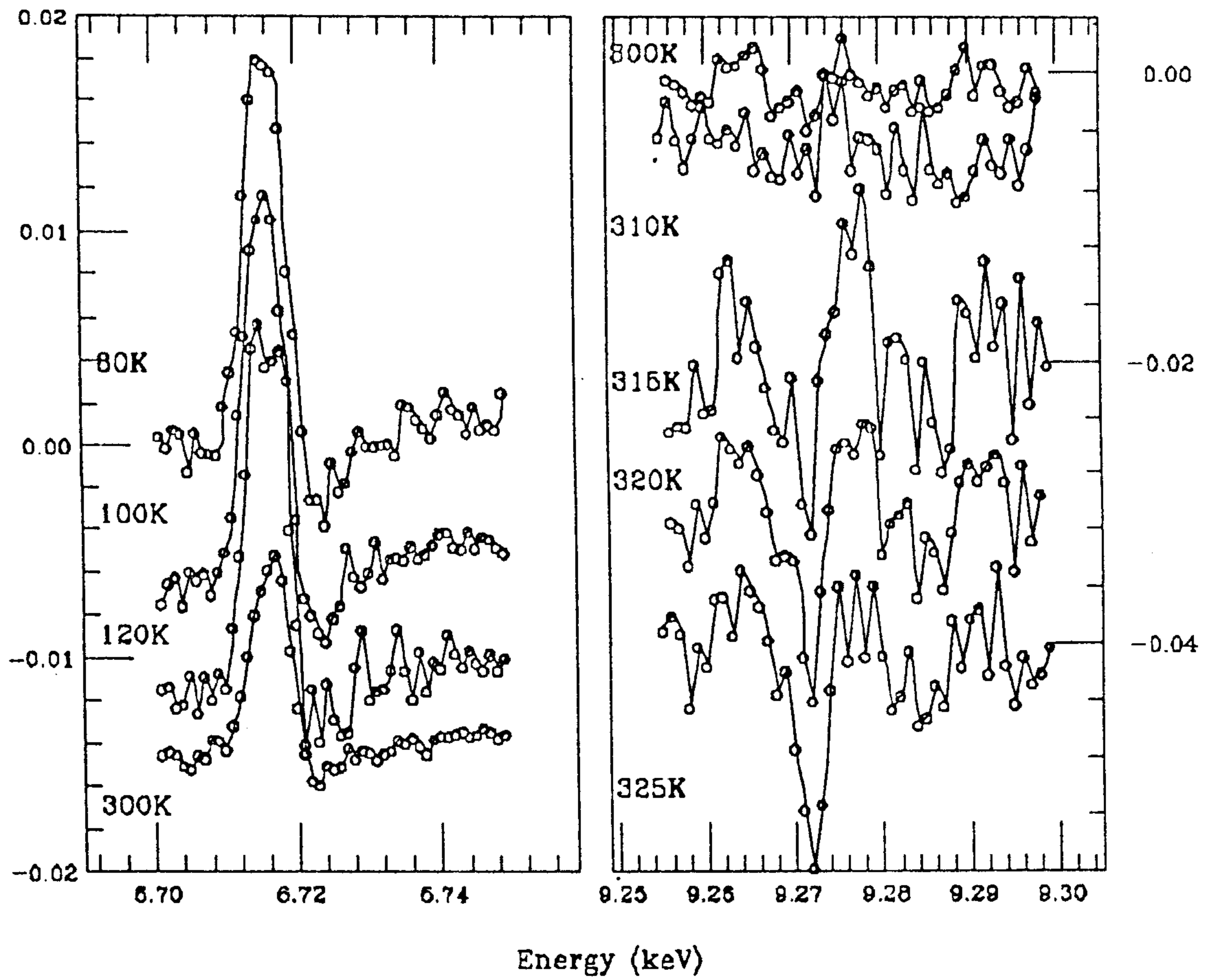


FIG. 2. Nd (left panel) and Er (right panel)  $L_2$ -edge XCMD signal recorded at different temperatures in  $Nd_2Fe_{14}B$  and  $Er_2Fe_{14}B$ , respectively.

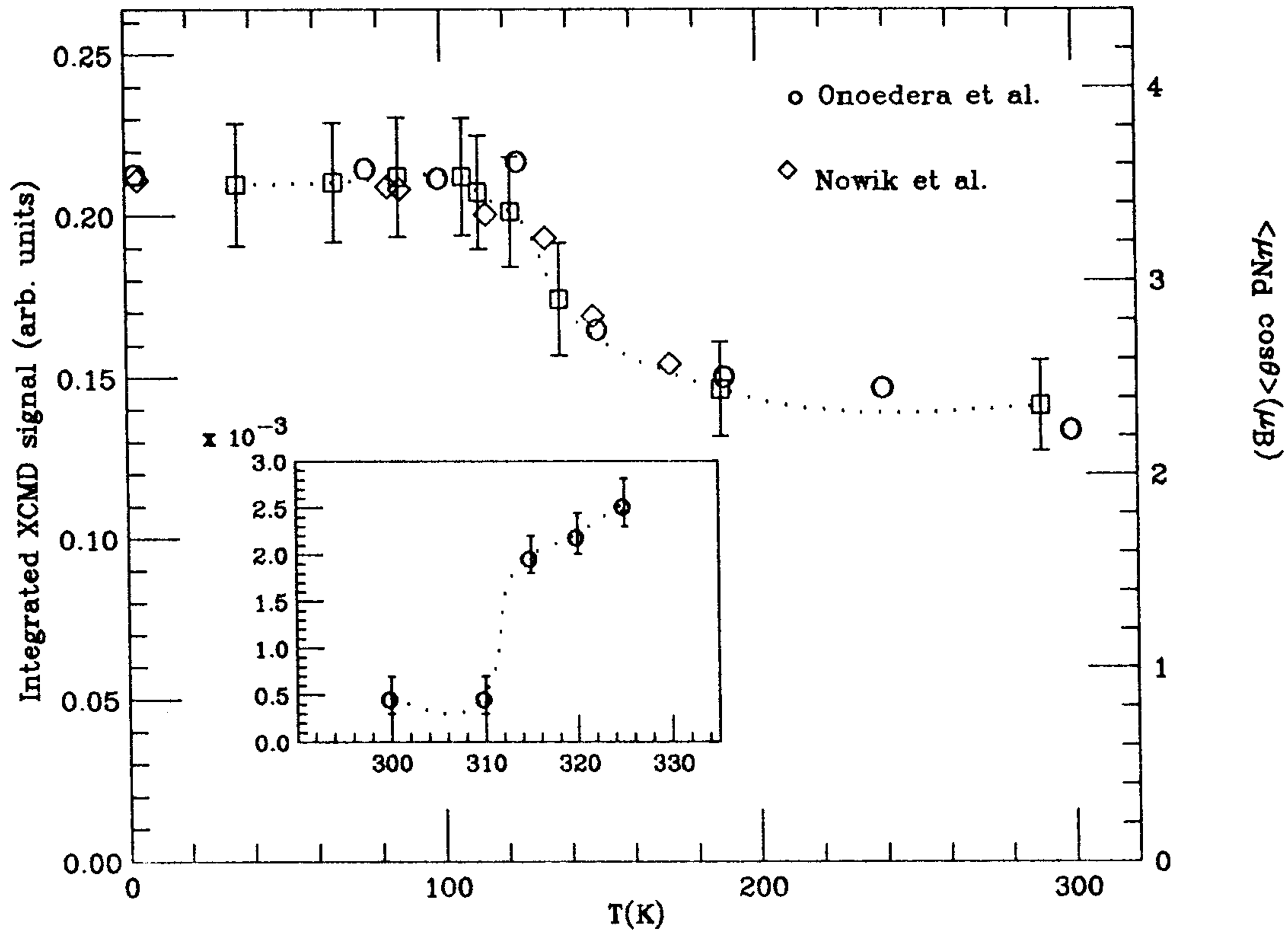


FIG. 3. Comparison between the temperature dependence of the the Nd  $L_2$ -edge integrated XCMD signal, ( $\square$ ), and the projection along the x-ray wave vector of the Nd magnetic moment taken from Ref. [3], ( $o$ ), and from hyperfine field values of Ref. [2], ( $\diamond$ ). The inset reports the temperature dependence of the Er  $L_2$ -edge XCMD integrated signal in  $Er_2Fe_{14}B$ .

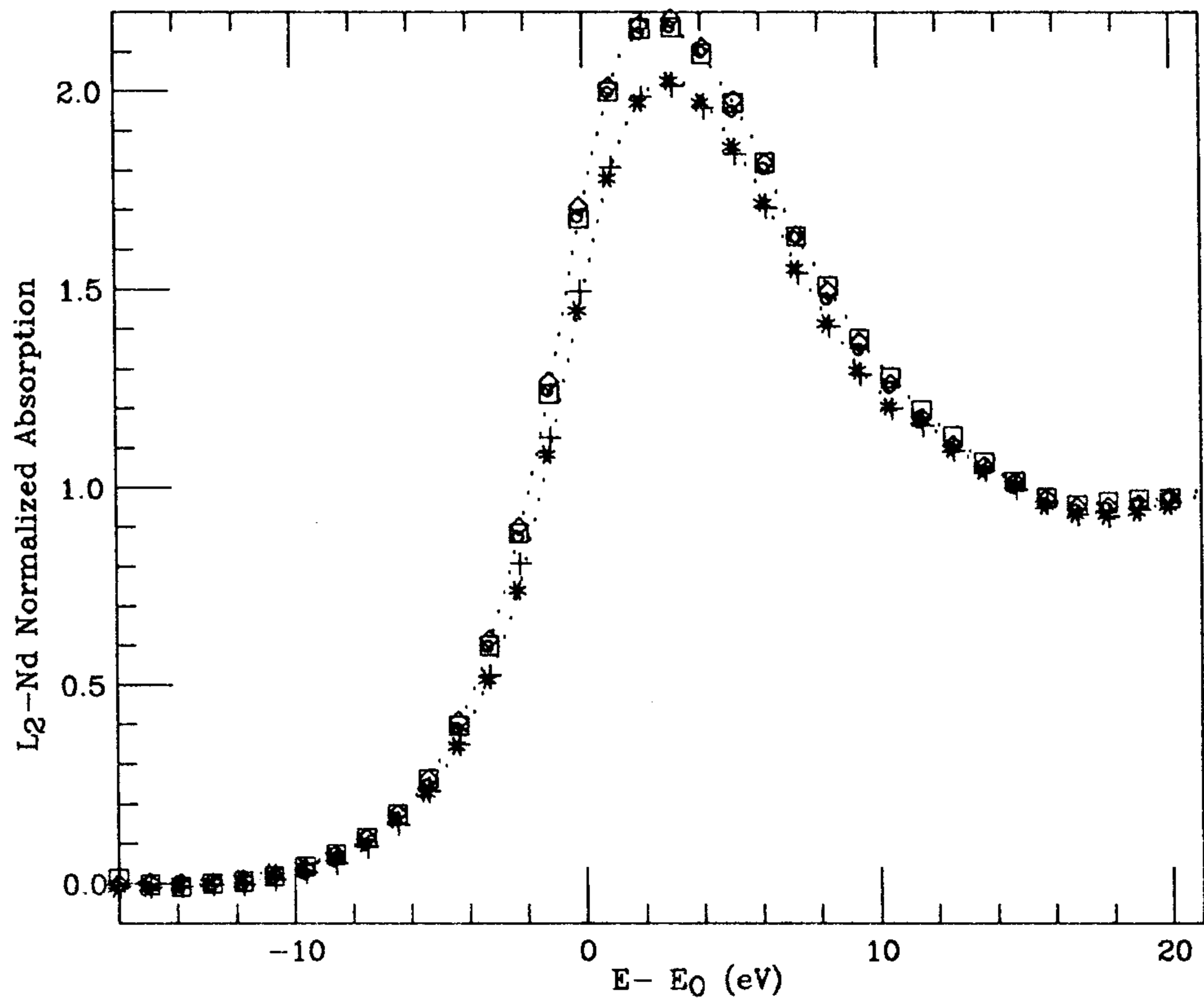


FIG. 4. The Nd  $L_2$ -edge XANES spectra in  $Nd_2Fe_{14}B$  at different temperatures: (\*)  $T=300$  K; (+)  $T=200$ K; ( $\square$ )  $T=120$  K; ( $\diamond$ )  $T=100$ K and ( $\circ$ ) 80K.